Ground Roll Dispersion Analysis at Springbank, Alberta

Dave G. Schieck and Robert R. Stewart

ABSTRACT

A three-component shallow reflection seismic line from Springbank, Alberta demonstrates large amplitude, surface wave noise due to the use of a surface energy source. Changes in phase velocity versus frequency, referred to as dispersion, of surface waves is primarily dependent on the shear wave velocities and thicknesses of the wave channels.

Shear wave refraction first breaks are picked from the radial or in-line shear wave shot records. These picks are inverted with for near-surface shear wave lithology. This enabled a dispersion model to be calculated which is used to identify and interpret surface wave noise on the shot record. By summing the ω-p wavefield transform of the vertical and radial component on a shot consistent basis the dispersion curve can be observed directly. The change in phase velocity with frequency can be approximated by a linear frequency modulated (LFM) wave over the frequency bandwidth of the Rayleigh waves.

An offset varying compression operator is cross-correlated with each trace in the shot gather before multi-channel filtering to remove linear dispersion. This reduces dispersed surface waves to a single aliased dip which is more easily removed by the 2-D median f-k filter. The output is then uncompressed by flipping the operator in time and again cross-correlating.

This hybrid multichannel filter is applied to a synthetic shot record contaminated with LFM noise at a bandwidth of 8-30hz with velocity bounds of 230-800 m/s. The f-k domain representation of the synthetic shot record has a single focused dip of 520 m/s after LFM compression. This enables better removal of dispersive noise by the multichannel filters such as the velocity f-k or median f-k.

This new filter is applied to the real three-component data set. The results indicate that the best way to minimize surface wave noise in shallow reflection studies is through careful choice of the acquisition parameters to ensure the target events are within the optimum offset window. In this example, the ground roll filtering is unable to recover the underlying reflection signals within the surface wave noise. The best CDP stack obtained for the P-wave data is due to an inside or near offset mute to completely remove the Rayleigh waves from the shot records before stacking.

INTRODUCTION

Rayleigh waves are the dominant surface waves recorded on the vertical and radial components of the seismic wavefield. These waves are non-dispersive in the classical case of propagation along the surface of an isotropic homogeneous half-space (Aki and Richards, 1980). In the real earth case of layered medium Rayleigh waves are dispersive and multiple modes are possible (Dobrin *et al*, 1951, Tolstoy and Usdin, 1953, Mooney and Bolt, 1966, Al Husseini *et al*, 1981).

Two important areas of study in exploration seismology are a direct result of this dispersive characteristic of surface waves. First, ground roll removal from the seismic record with dispersion phase match filters (Beresford-Smith and Rango, 1988, Saatçilar and Canitez, 1988, and Herrmann *et al*, 1990). Second the inversion of dispersion curves for near-surface S-wave lithology (Mari, 1984, Russell, 1987, Gabriels *et al*, 1987, Szelwis and Behle, 1987, Wattrus, 1989, and Glangeaud, 1990). Both applications are improved by the wavefield transformation ω-p, a 1-D Fourier transform in τ of the τ-p slant stack (McMechan and Yedlin, 1981). The spectral peak of this frequency-slowness domain gives the frequency associated with each phase velocity or the dispersion curve of a multi-channel record directly.

The frequency range of Rayleigh waves ($\approx$4-25 Hz) is within the frequency bandwidth of P-SV wave data (typically 8-35 Hz) data thus precludes the use of narrow-band filters or deconvolution to suppress or remove them without degrading the reflections. In P-wave conventional recording it is standard practice to use geophone arrays which attenuate non-vertical wave motion such as ground roll. The desired P-SV wave motion is also attenuated by these receiver arrays, hence, the general use of single or nested geophones for multi-component recording.

The offset range where target P-wave reflections arrive before the earliest Rayleigh waves on a vertical component record is often referred to as the optimum offset window in shallow reflection seismology (Hunter *et al*, 1984). Figure 1 (a)) shows that between the "first arrivals" of the refracted P-wave (RFp) and the ground roll there is a favourable P-wave reflection window for events **A** and **B** to be adequately recorded. The velocities of shear waves are very close to the velocity of Rayleigh waves particularly in the near surface where Poisson's ratio is usually higher than 0.4 (Knopoff, 1952). Therefore source generated shear waves which are refracted (RFs) in the near surface arrive only slightly before the ground roll. P-SV wave reflections typically are delayed by 1.5 times their associated P-wave reflections (assuming Vp/Vs=2) so events **A** and **B** will often be contaminated with large amplitude Rayleigh wave noise (Figure 1 (b)).

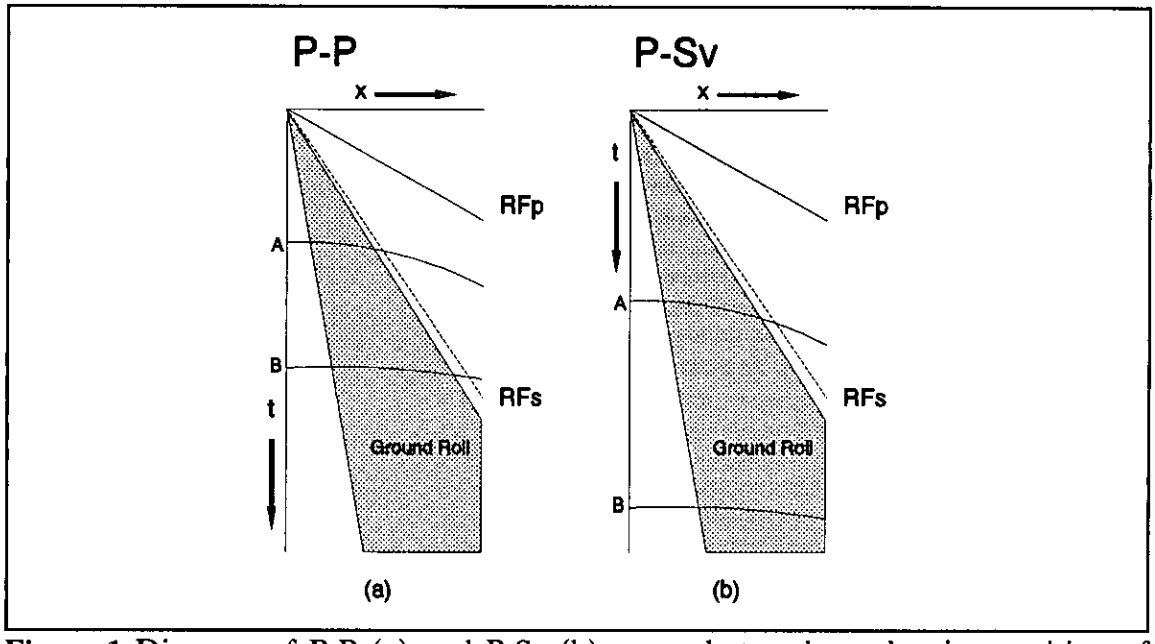

Figure 1 Diagram of P-P (a) and P-Sv (b) wave shot gathers showing position of refracted arrivals (RFp and RFs), ground roll window, and reflection events (A&B). x is distance and t is time.

Due to low energy sources or limitations in recording parameters (ie. limited number of channels for 3-C data) the optimum window may not be available at the target depth for shallow reflection seismology. A robust, efficient method must be developed to obtain the required reflection signals from within the large amplitude surface wave window. In this study a linear approximation of the dispersion curve over limited frequency bandwidth and velocity bounds is used to develop a ground roll compression operator. Previously, it was found that a pre-stack median f-k filter removes aliased dips if they appear as noise spikes within the local weighted median window (Schieck and Stewart, 1990). Compression of the dispersed ground roll is necessary to optimize this localized non-linear filter.

METHODS

To understand the effects of near surface lithology on the dispersion of ground roll a simple near surface model was established (Figure 2). The matrix method is used to integrate the Rayleigh-wave equations and assumes that the model is represented by a stack of homogeneous isotropic layers (Takeuchi and Saito, 1972, Schwab and Knopoff, 1972). These methods require further refinements at the higher frequencies needed in exploration seismology (Abo-Zena, 1979), specifically, when the thickness of a layer is greater than several wavelengths. Recently, public domain algorithms have been made available to calculate phase velocity versus frequency or dispersion curves for multiple layers in the near-surface (Doornbos, 1988).

The model parameters density, thickness, P- and S-wave velocities for the weathering and drift layers of figure 2 are perturbed by a factor of 20% to demonstrate the importance in affecting the dispersion of ground roll. Figures 3 and 4 depict only a minimal dependence of dispersion on P-wave velocities and densities.

Further these curves are bounded at lower frequencies by the underlying S-wave velocities and at higher frequencies by the surface wave propagating matrix velocities (Figure 5 and 6). Finally, a thicker propagation layer causes a steeper dispersion curve (Figure 7) and thinner layers cause the curves to move to higher frequencies. In the limit of an infinitely thick layer, relative to wavelength, a non-dispersive phase velocity-frequency curve will result. Note also that for limited low frequency response of geophones the primary modes of dispersive surface waves may not be observed resulting in higher frequency or higher modes of the same velocity bound dispersion curve (Mooney and Bolt, 1966). Clearly the shape of the dispersion curve is primarily dependent on the near-surface shear wave velocities and thicknesses.

If the slope of the dispersion curve can be approximated by a line a very simple phase match filter can be used to compress the dispersion to a bandlimited spike. A linear frequency-modulated wavelet l(t) is given by

$$l(t)=\cos(\omega_c t+\frac{\Delta\omega}{2T}t^2), \qquad -\frac{T}{2}\le t\le\frac{T}{2} \qquad (1)$$
$$=0, \qquad \textit{otherwise.}$$

where T is the time length of the wavelet, ω_c is the carrier frequency and $\Delta\omega$ is the modulation bandwidth (after Saatçilar and Canitez, 1988).

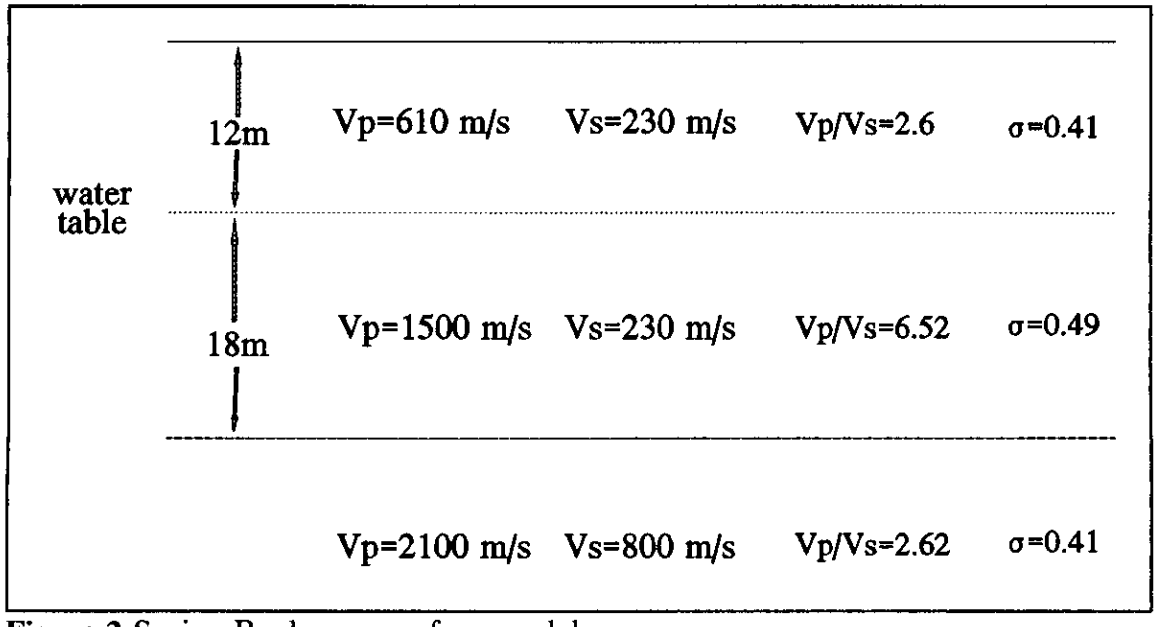

Figure 2 Spring Bank near surface model

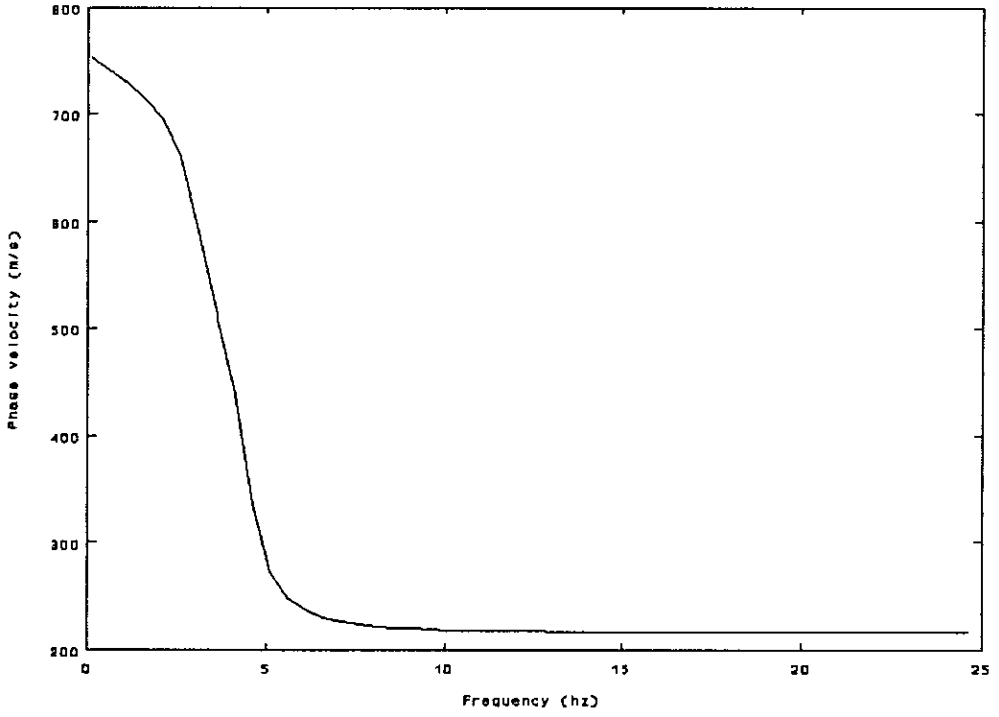

Figure 3 Rayleigh wave dispersion curves for varying densities.

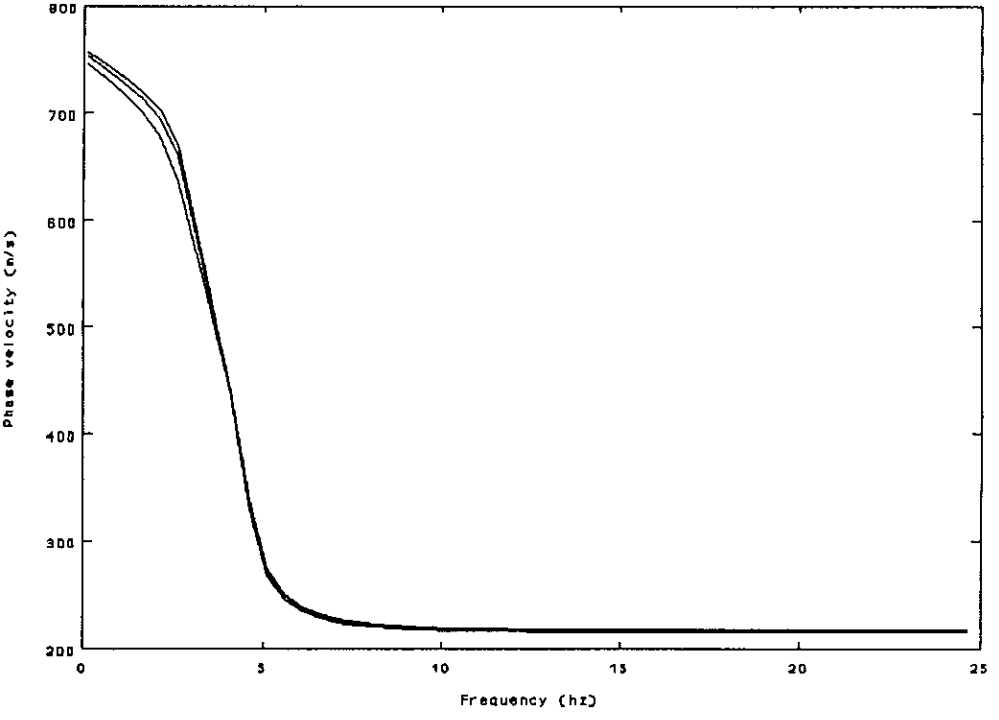

Figure 4 Rayleigh wave dispersion curves for varying P-wave velocities.

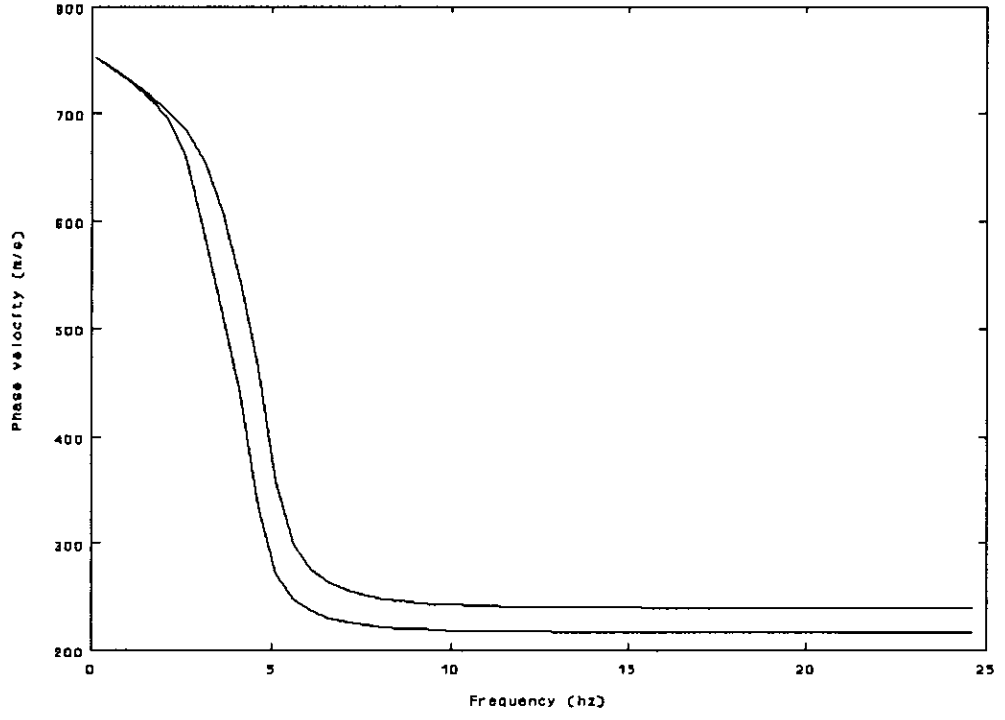

Figure 5 Rayleigh wave dispersion curves for varying S-wave velocity in first layer.

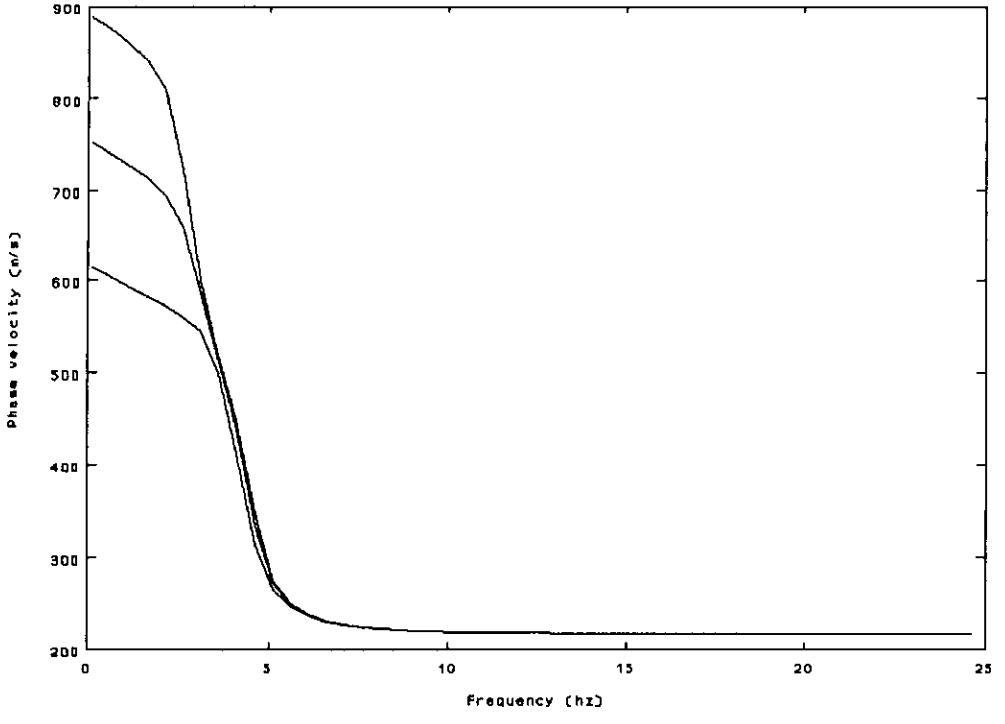

Figure 6 Rayleigh wave dispersion curves for varying S-wave velocity in second layer.

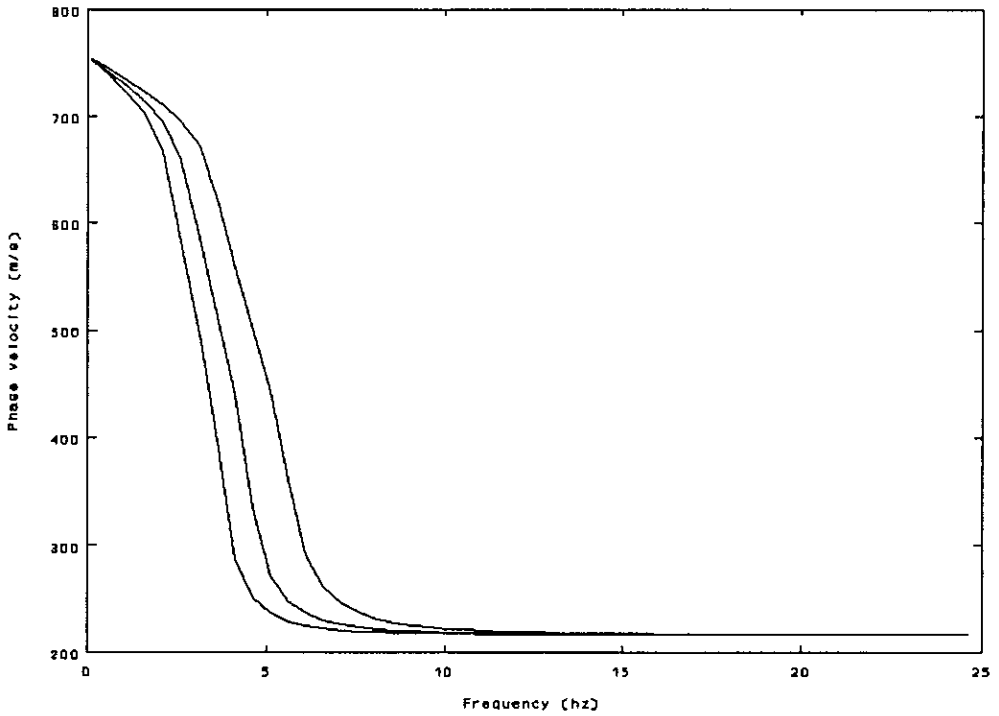

Figure 7 Rayleigh wave dispersion curves for varying thicknesses.

The Fourier transform of w(t) is

$$L(w)=|A_L(w)|e^{-i(\phi_0+\phi(w))}, \tag{2}$$

where

$$\phi(\omega)=\frac{-\Delta\omega T}{2}\left(\frac{\omega_c-\omega}{\Delta\omega}\right)^2 \tag{3}$$

and ϕ_0 is the initial phase. The match filter mf(t) to this wavelet is simply a time reversed, time-delayed (Γ), and scaled version of the wavelet as

$$mf(t)=k*l(\Gamma-t). \tag{4}$$

Neglecting the time delay and using a scaled amplitude equal to 1.0 the Fourier transform of the match filter is

$$MF(\omega)=L^*(\omega)=|MF(\omega)|e^{i\left[\frac{\Delta\omega T}{2}\left(\frac{\omega_c-\omega}{\Delta\omega}\right)^2\right]} \tag{5}$$

where L^* is the complex conjugate of the Fourier transform of l(t) (Turin, 1960).

The match filter is designed in the frequency domain and its amplitude spectrum is set to unity over the frequency bandwidth of the signal. This assures that the inverse application of this filter after multi-channel f-k or median f-k filter does not affect the amplitude spectrum of the data. Figure 8 depicts an operator with amplitude equal to the phase spectrum frequency bandwidth of 8-30 hz. Figure 9

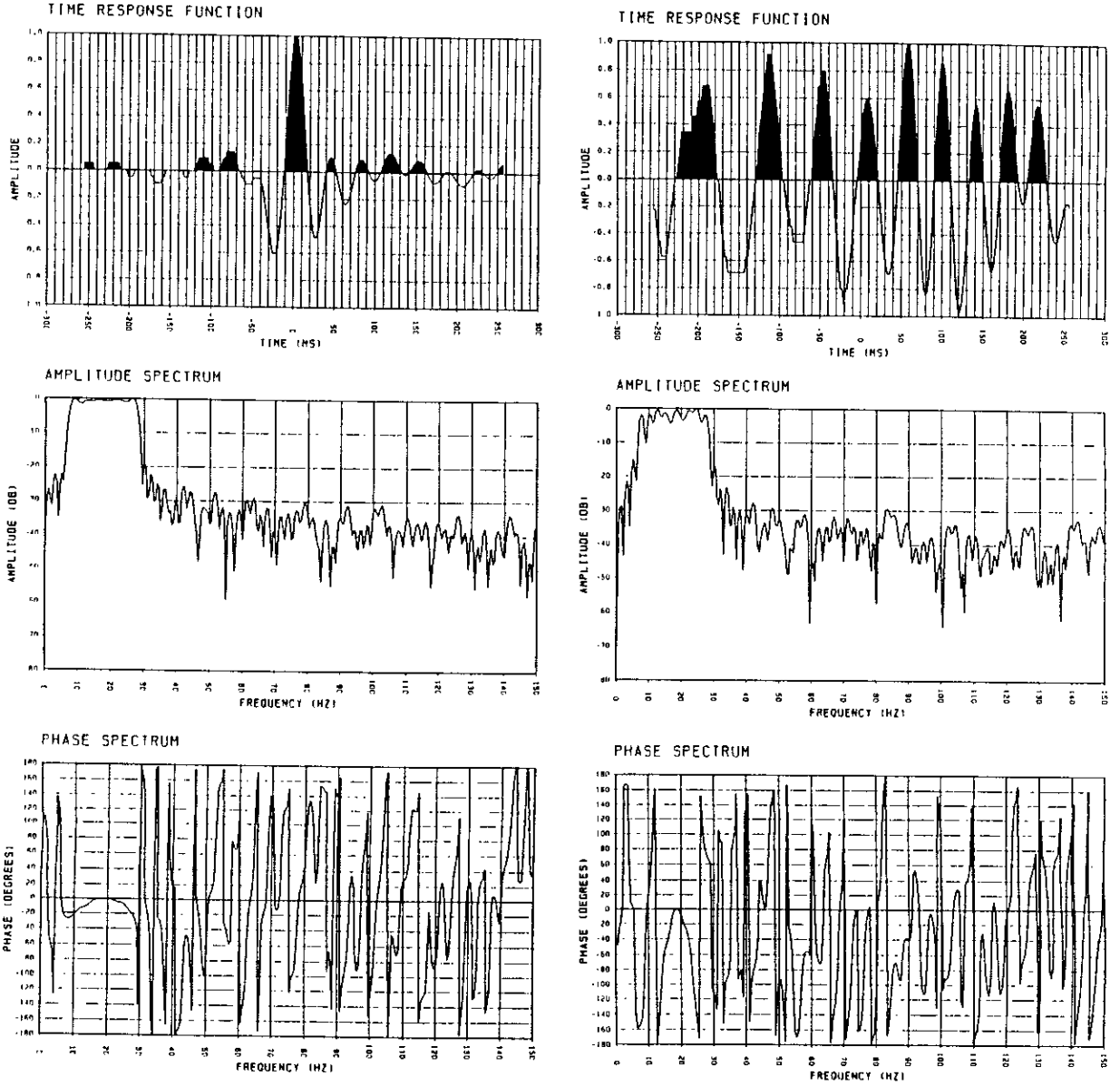

Figure 8 LMF filter operator with frequency bandwidth equal to the bandwidth of the phase a) x = 10 m, and b) x = 160 m.

shows an operator with a phase compression bandwidth of 8-30 hz but an increased amplitude spectrum of 8-70 hz.

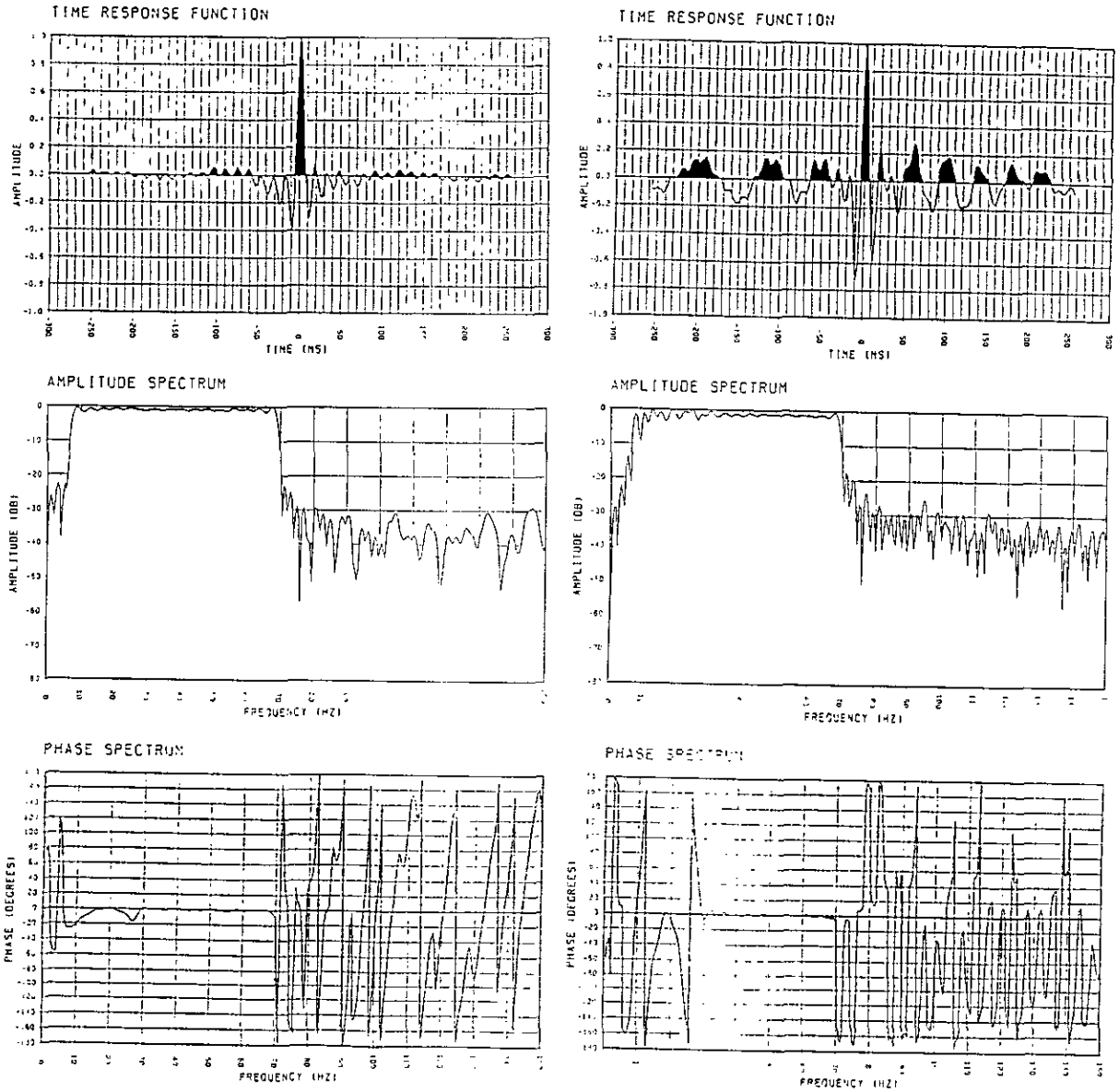

Figure 9 LMF filter with amplitude spectrum bandwidth of 8-70 hz and phase compression over 8-30 hz a) x = 10 m and b) x = 160 m.

For increasing offsets (x) the time duration of the LMF will increase and is limited at low frequencies by the second layer velocity (V_2) and at higher frequencies by the propagating layer velocity (V_1). Equation (5) becomes

$$MF(\omega)=L^*(\omega)=|MF(\omega)|e^{i[\frac{x}{2\Delta V}\frac{(\omega_c-\omega)^2}{\Delta\omega}]} \qquad (6)$$

where ΔV is the difference in velocity.

Dziewonski and Hales (1972) define phase velocity as the instantaneous velocity of plane waves at a given frequency as

$$c(\omega)=\frac{dx}{dt}=\frac{\omega}{k(\omega)} \tag{7}$$

and the group velocity as the velocity of transmission

$$u(\omega)=\frac{x}{t}=\frac{d\omega}{dk}=c(\omega)+k(\omega)\frac{dc(\omega)}{dk(\omega)}. \tag{8}$$

The assumption of measuring surface waves with sums of plane waves is generally valid at large distances from the source (Aki and Richard, 1980). Only by assuming a single propagating mode can the phase velocity be determined directly from the phase of the 2-D Fourier transform. Generally, there can be an infinite number of wavenumber (k) solutions or modes to the equation of motion for Rayleigh waves so a robust method to isolate individual normal modes of propagation is required.

The phase between two stations, in the same plane as the source, is represented by $k_m(\omega)\Delta x$, where Δx is the distance between stations. If $k_m(\omega)$ is identified correctly, the phases of a propagating mode can be aligned and summed at a maximum. Equation (7) can be re-written as

$$k_m(\omega)=\frac{\omega}{c_m(\omega)}=\omega p(\omega) \tag{9}$$

where $p_m = 1/c_m$ is slowness. The slant stacking wavefield transformation of McMechan and Yedlin (1981) yields these modes directly by first mapping the data to τ-p then by way of a Fourier transform in τ to ω-p. If the slowness is approximately a linear function of frequency the ground roll is linearly modulated. Also, the frequency band of the desired compression operator can be measured directly.

RESULTS

The 3-component field data (FS91-1) was recorded in August, 1991, and starts 250m from the previous years 2-component data (FS90-1) to the east (refer Figure 8). A Betsy 8-gauge seisgun shot at the surface was the energy source. This generated

a good deal of surface wave energy on all three recorded components. The field parameters for this line are:

Number of traces:	32
Station interval:	10 m
Geophones:	3-C Oyo, 10 Hz
Minimum offset:	10 m
Maximum offset:	160 m
Instruments:	Sercel 338HR
Sample interval:	2 ms
Record length:	1 s
Fold:	32

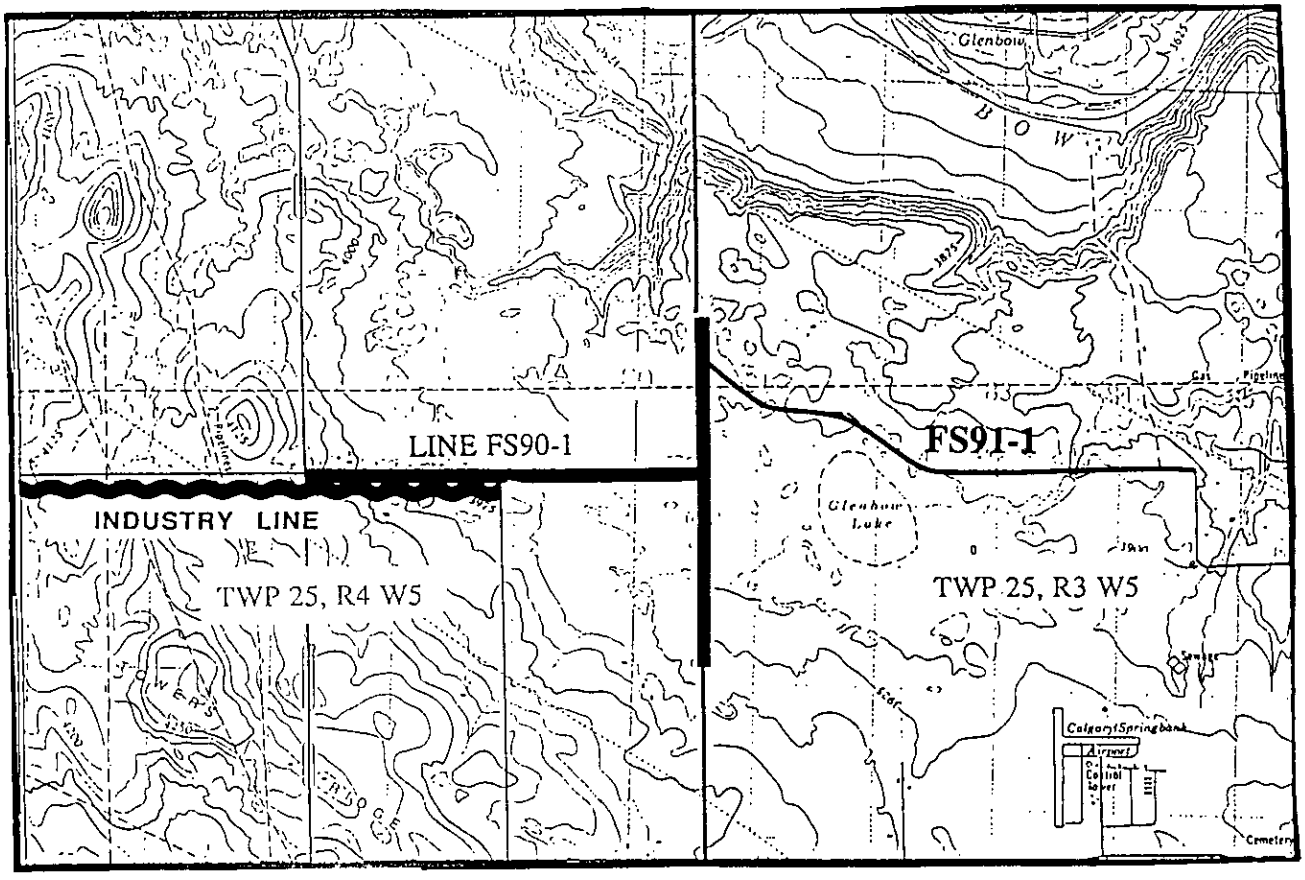

Figure 10 Spring Bank map showing locations of seismic lines FS90-1 and FS91-1.

Figure 18 shows a typical P-wave and P-Sv wave shot record with a series of narrow band filter panels. The frequency bandwidth of the surface waves on both components is 4-50 hz. These higher frequencies suggest that higher modes of the Rayleigh waves are present. The S-wave refraction first breaks were reasonably pickable on an interactive workstation. The P-wave and S-wave first breaks were inverted with an interactive GLI refraction analysis package. The interpreted first breaks are depicted in figures 11 and 12. A model (Figure 2) to generate the synthetics and later infer parameters of the LFM compression operator was established.

To investigate the effect of the LFM compression operator on the multi-channel f-k and median f-k filters a synthetic shot gather with linear frequency modulated surface waves was generated. The frequency bandwidth of the ground roll was 8-30 hz and the reflections 10-60 hz (Figure 13). The compression operators from figure 9 were convolved before the multi-channel filters and compared to the results of applying these same filters without compression. The median f-k benefits from the surface wave compression primarily due to its ability to remove isolated aliased dips. The f-k domain results depicted in figures 14 and 15 demonstrate the effectiveness of the LFM filter in enhancing both multi-channel fan filters.

After determining the shear wave velocity bounds from the refraction analysis the shot gathers were transformed to the ω-p domain. A factor of $\sqrt{x}$ was used to compensate for geometric spreading. A slant stack from 0-90 ms/trace moveout at 160m offset was followed by a 1-D Fourier transform in τ to obtain the ω-p stack. This process was applied to both the radial and vertical channels and their subsequent amplitude spectrums were summed together to minimize noise (Figure 16). Within the velocity bounds and on the basis of expected linear slopes determined from the dispersion models (Figure 7) the LFM operator is shown as a sloping line on the ω-p plots. Further confirmation of this estimate was gained by measuring the apparent velocities of the surface waves of the narrow band filter panels of figure 18.

The frequency bandwidth of the data is approximately 4-70 hz while the LFM slope is 17-25 hz. This means a Δf of 9 hz and a phase velocity bounds of 230 to 800 m/s. The maximum time duration (T) of the dispersive wave train occurs at the maximum offset of 160m and is simply 280 ms. A 512 ms operator is designed in the frequency domain at each offset and applied as a 1-D cross-correlation time domain operator. By designing the phase and amplitude spectrums independently then inverse transforming to time the phase match filter will pass all signal frequencies while compressing the dispersive waves only over their limited bandwidths (Figure 17).

After LFM compression, pre-stack filters were applied to reject dips > 8 ms/trace. The LFM operators were flipped in time and again cross-correlated to return the reflected events to their original wavelet shape. Figure 19 compares the resultant common offset stacks for the unfiltered and pre-stack filtered gathers. The previous years two-component line (FS90-1) indicated primary reflectors should be seen as the Edmonton at 400 ms, an upper detachment at 700 ms and a lower detachment at 800 ms (Lawton and Harrison, 1990).

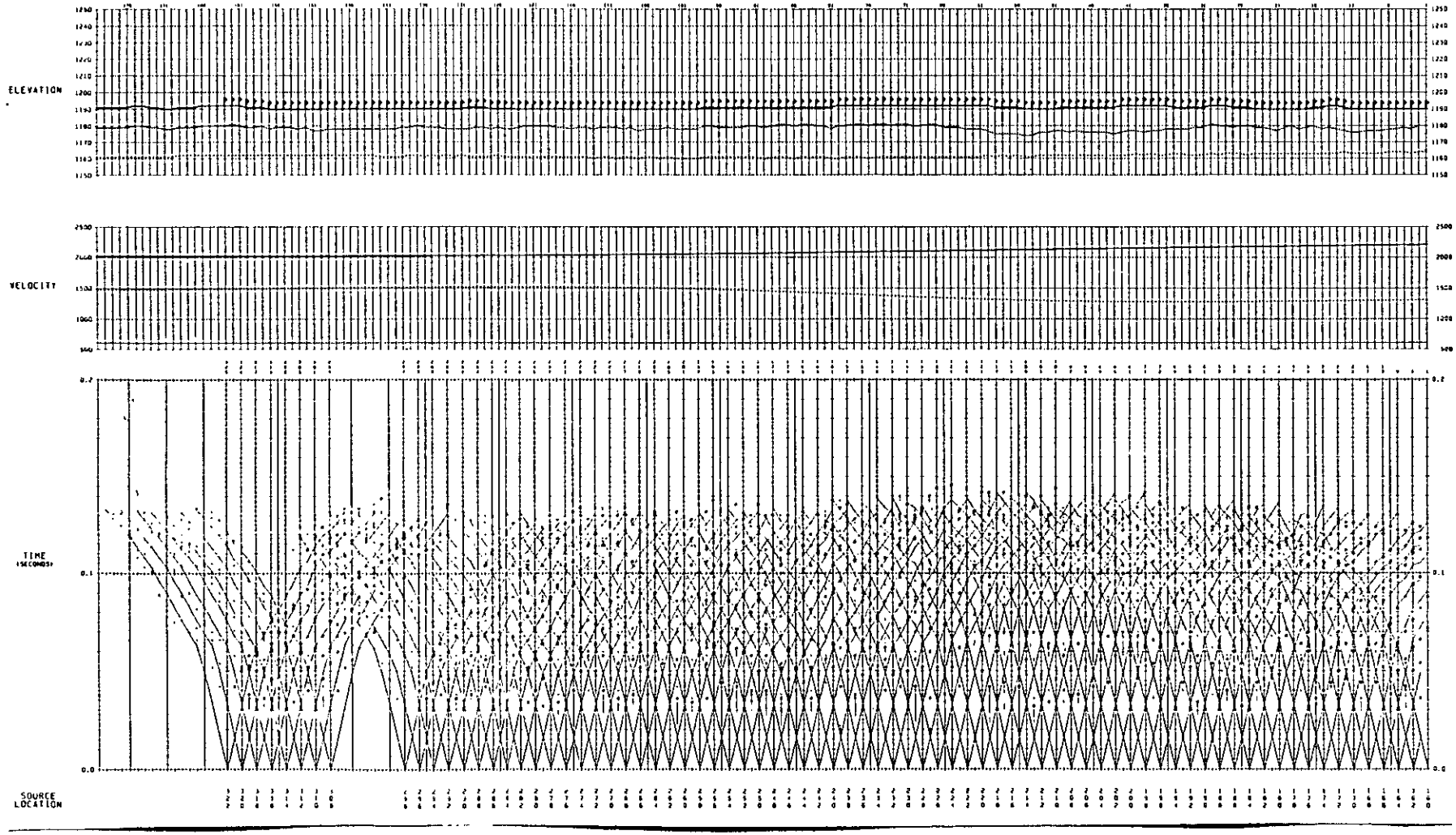

Figure 11. P-wave refraction first break picks, interpreted near surface velocities and thicknesses.

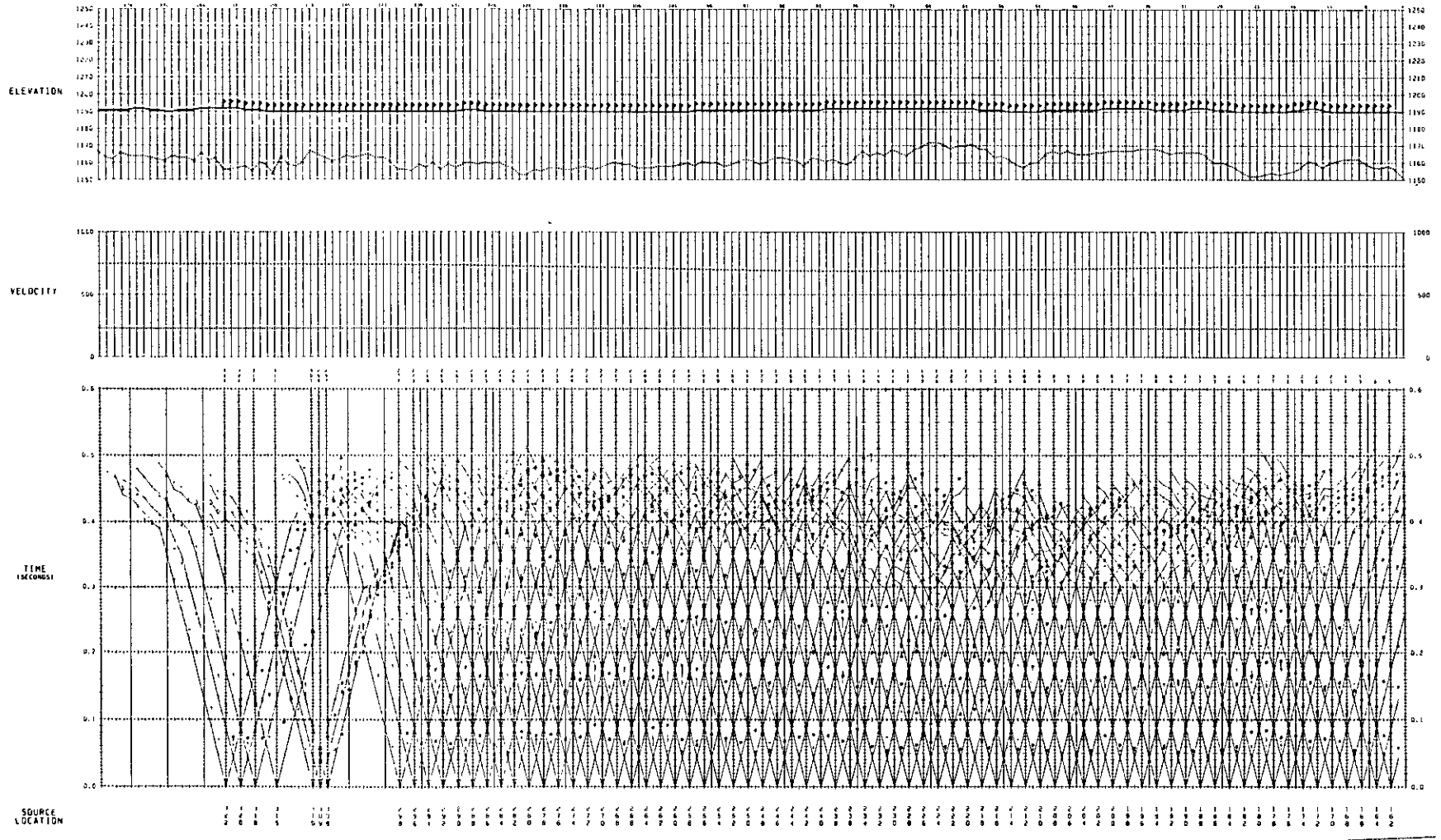

Figure 12. S-wave refraction first break picks, interpreted near surface velocities and thicknesses.

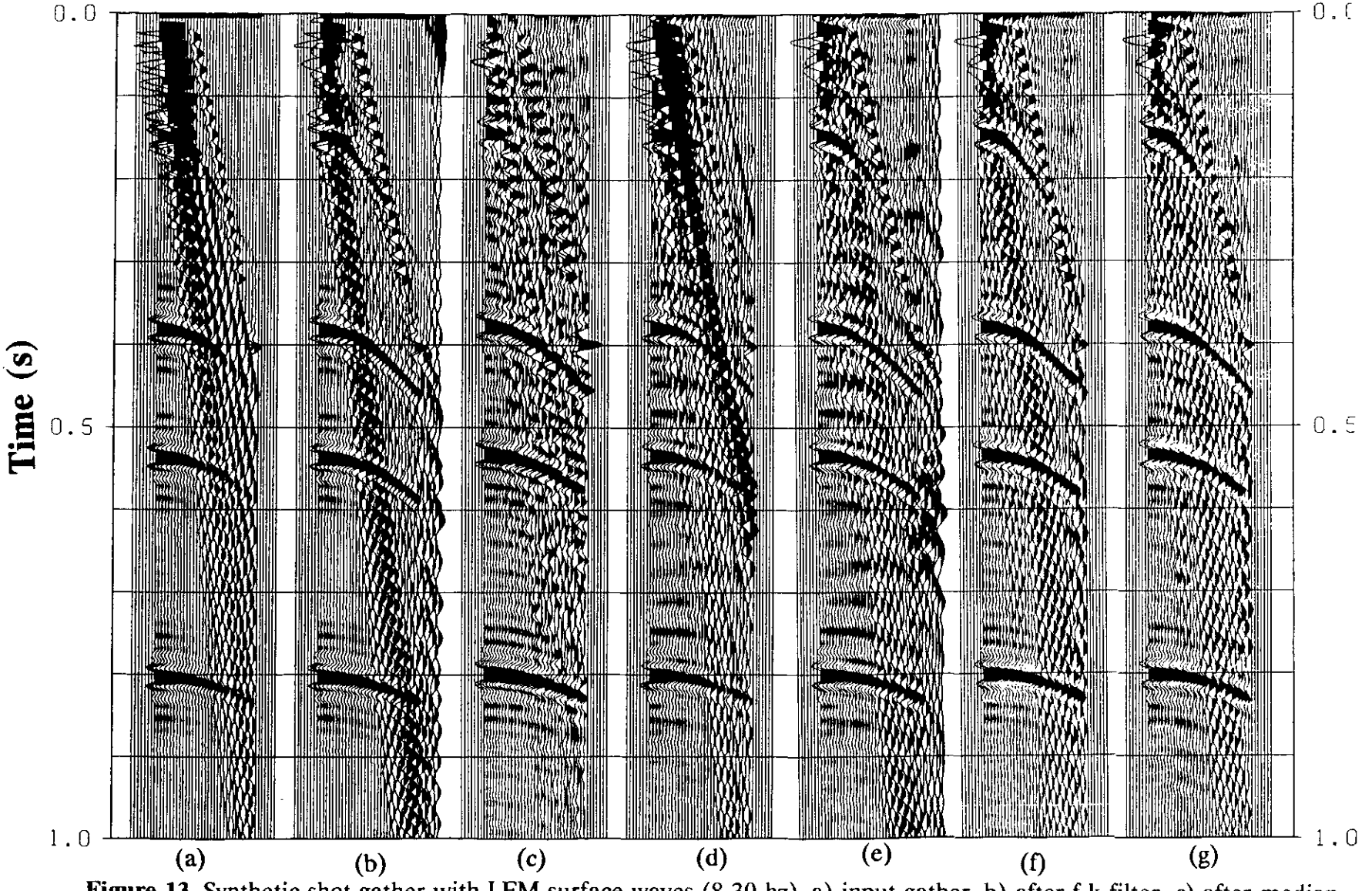

Figure 13. Synthetic shot gather with LFM surface waves (8-30 hz). a) input gather, b) after f-k filter, c) after median f-k filter, d) after LFM compression, e) f-k filter applied to d), f) LFM decompression of e), and g) median f-k as in f).

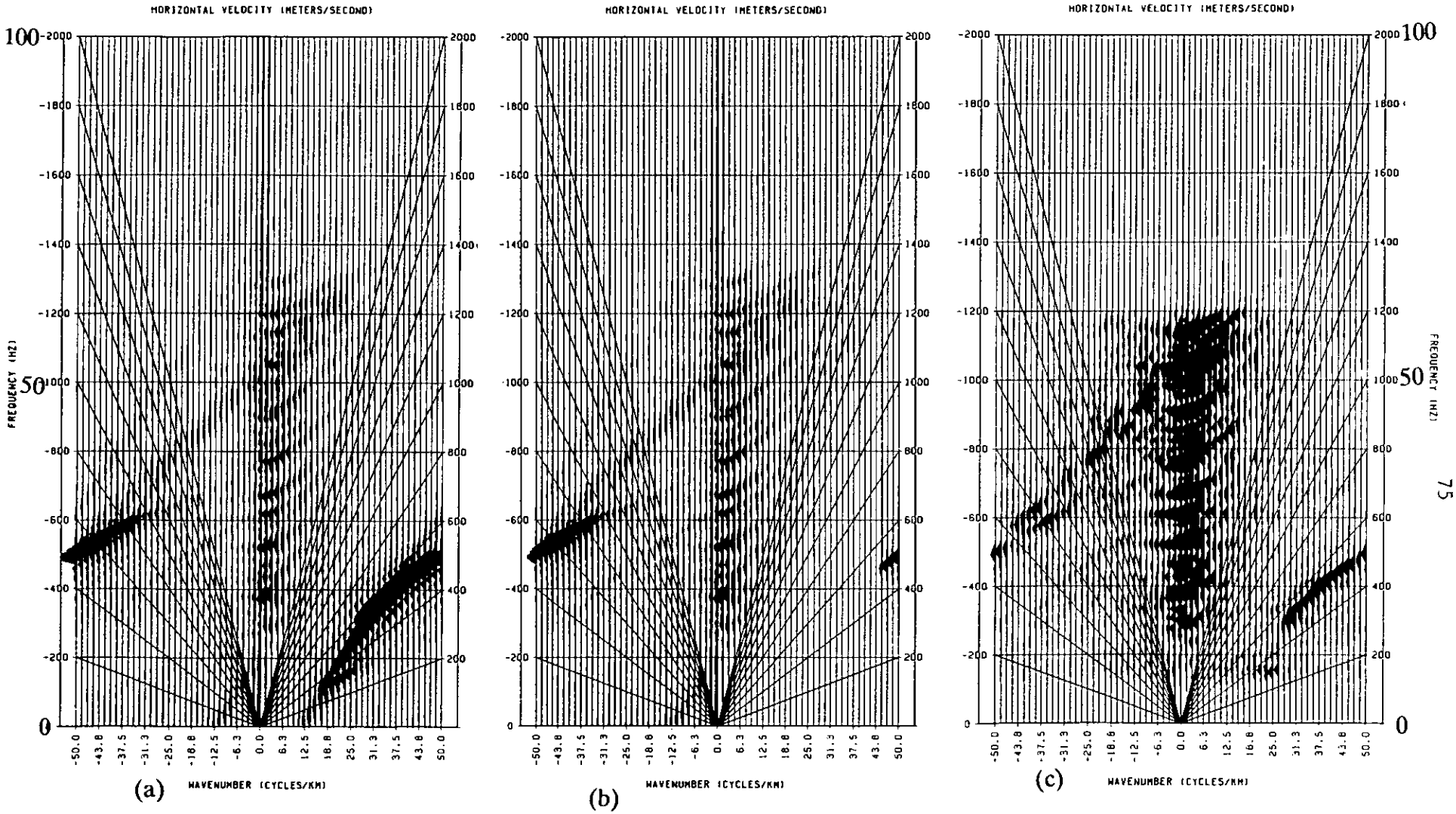

Figure 14 f-k transform of synthetic shot gather a) input gather, b) f-k filter (without LMF compression), and c) median f-k (without LMF compression).

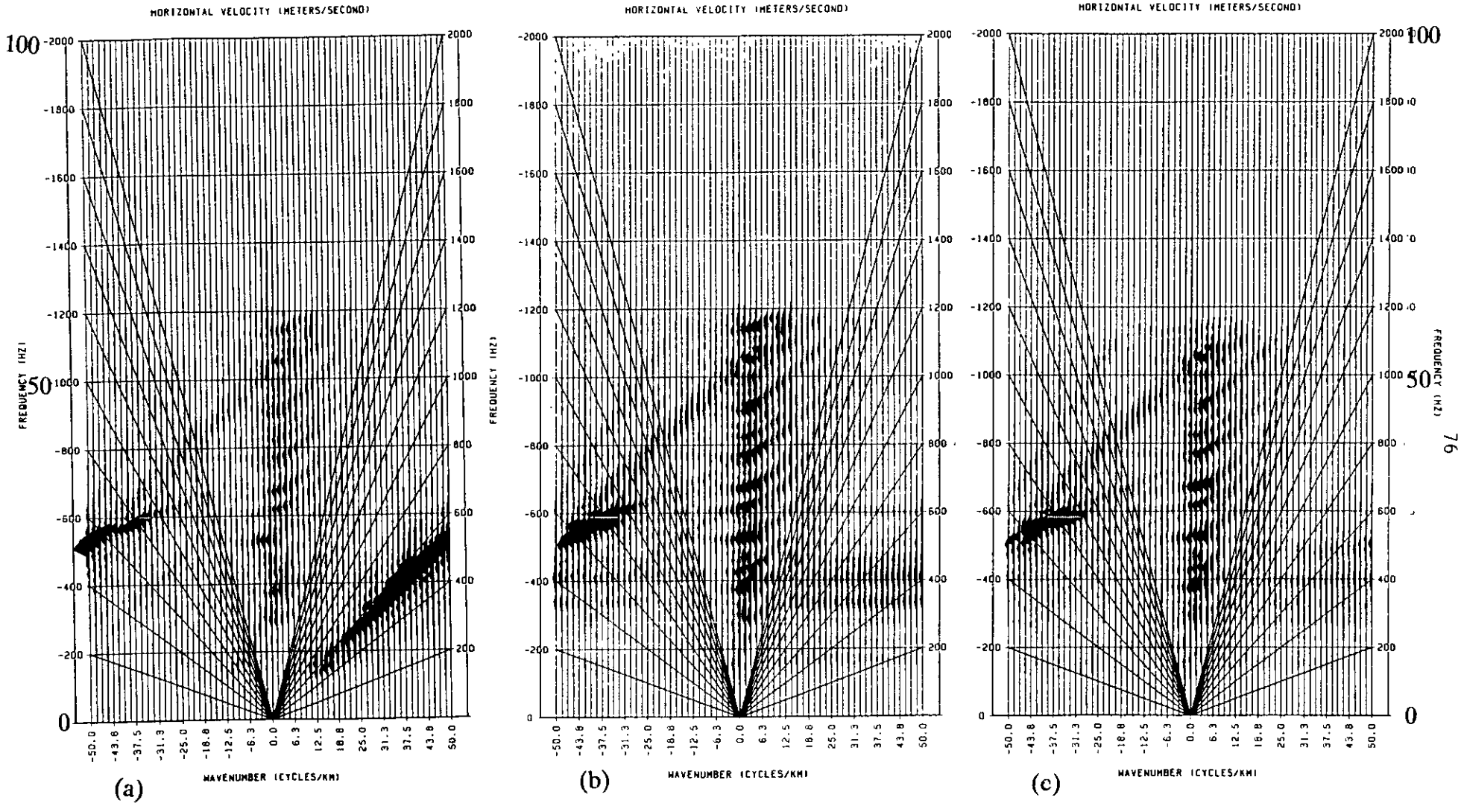

Figure 15 f-k transform of synthetic shot gather a) input gather after LMF compression, b) f-k filter (with LMF compression/de-compression), and c) median f-k (with LMF compression/de-compression).

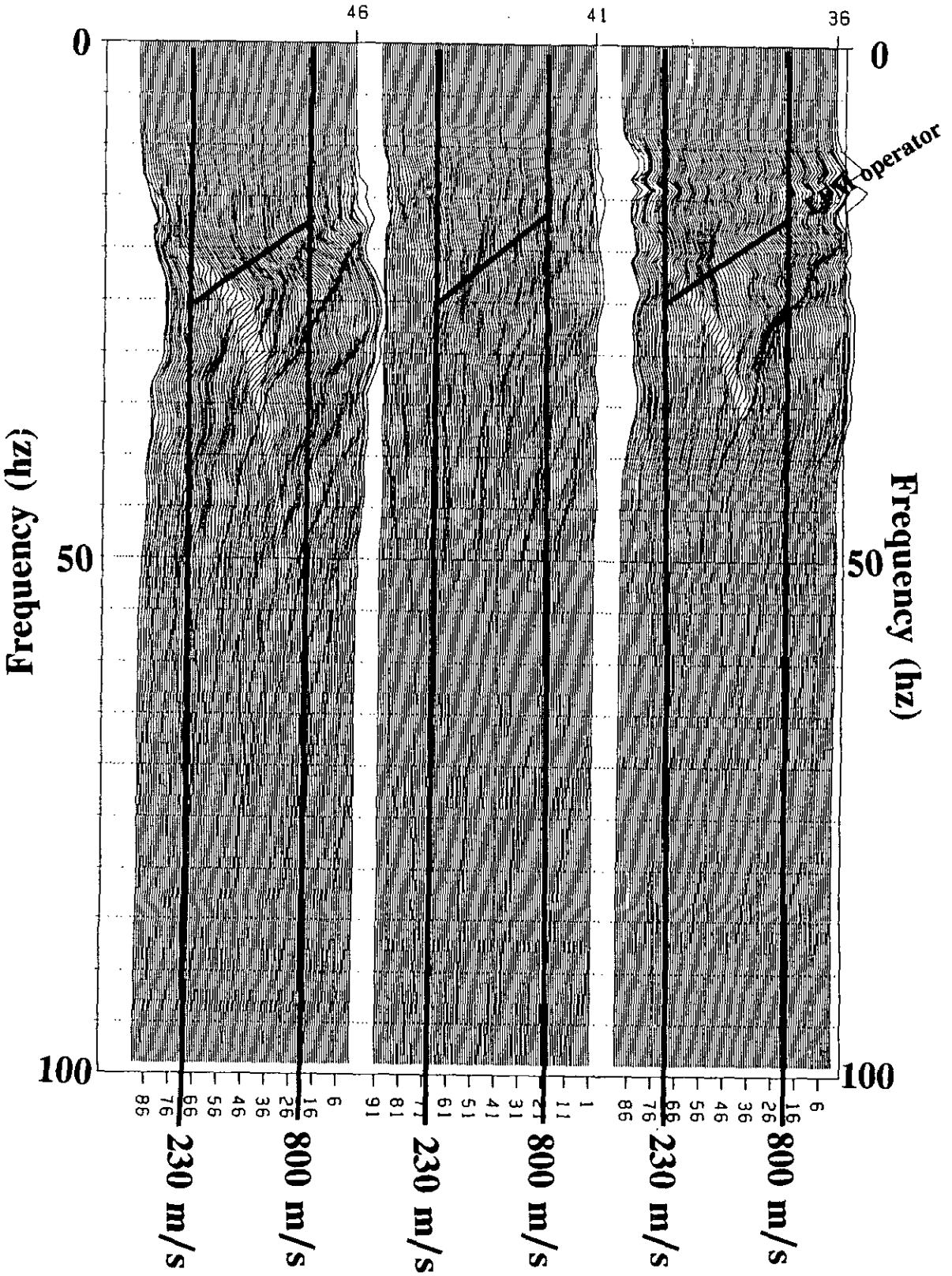

Figure 16 ω-p mapping of shot gathers 36, 41, and 46.

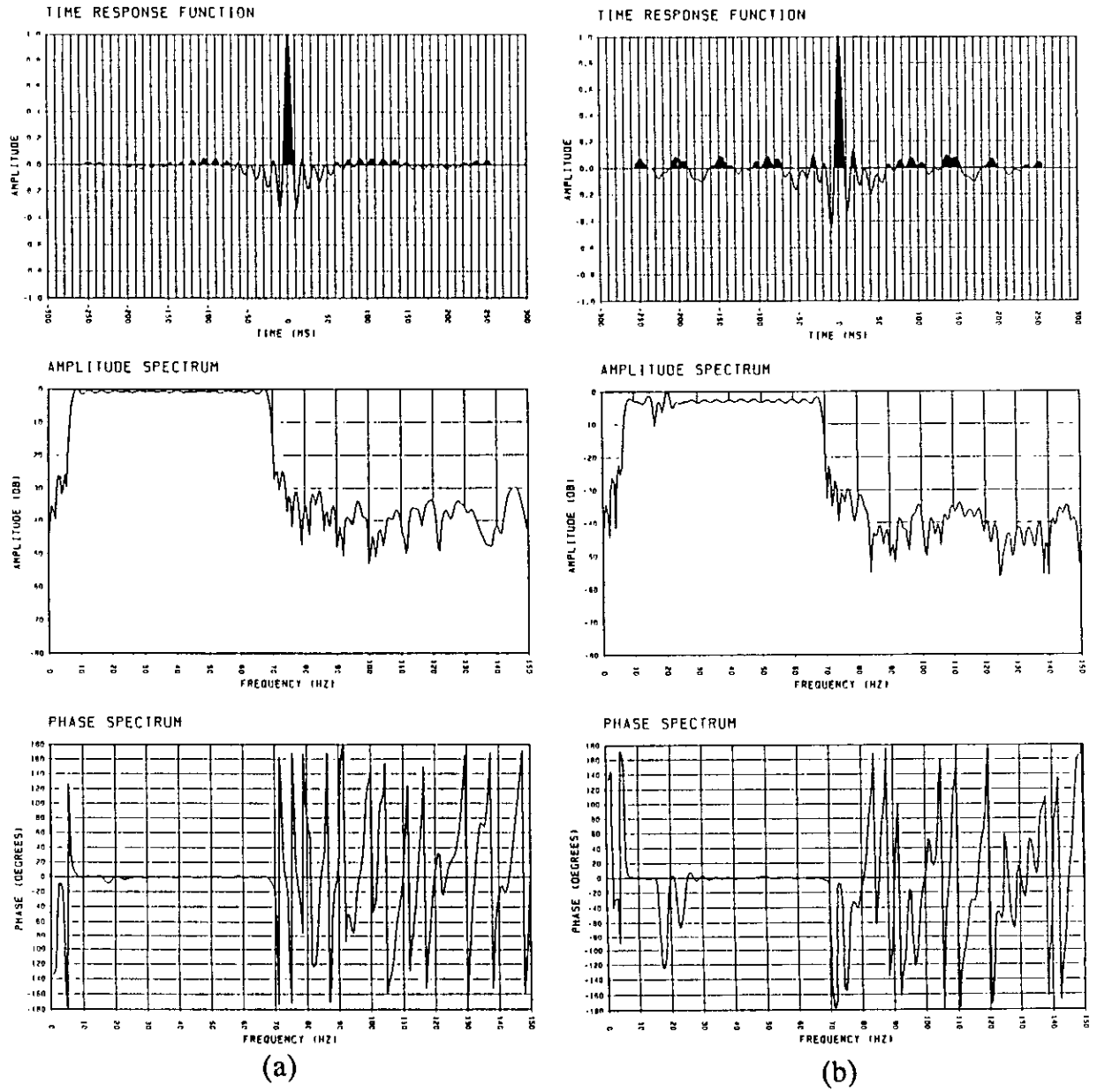

Figure 17 Ground roll compression operators a) x = 10, b) x = 160 m.

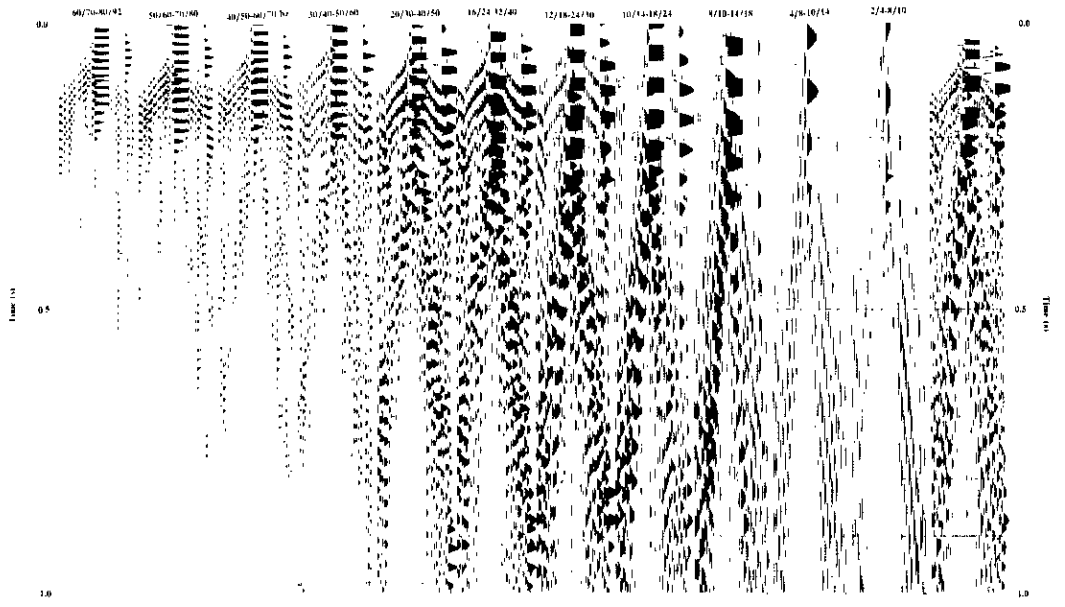

(a)

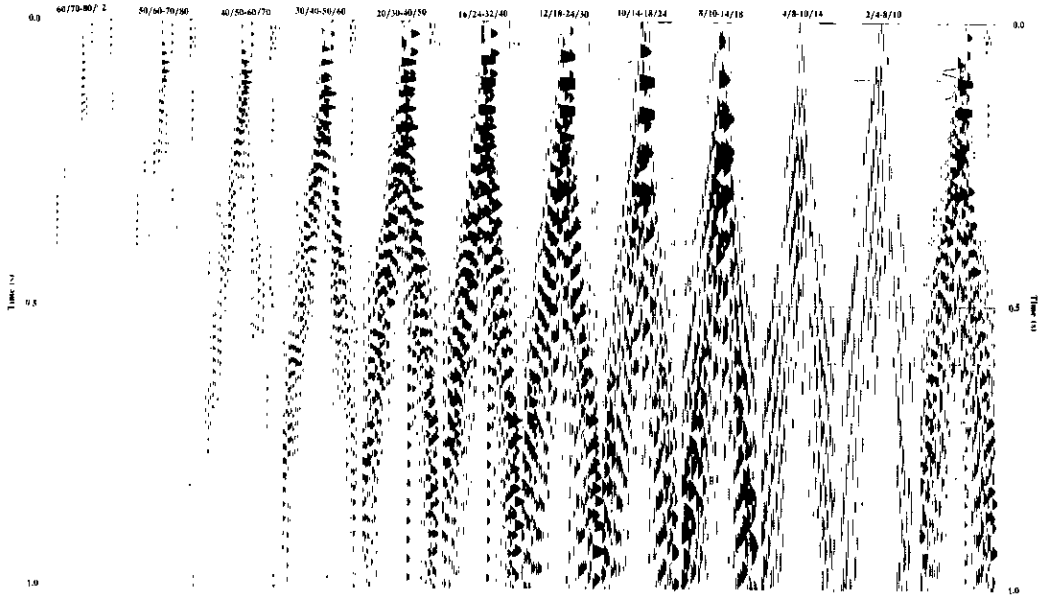

(b)

Figure 18 Shot point 41 a) vertical component, b) radial component.

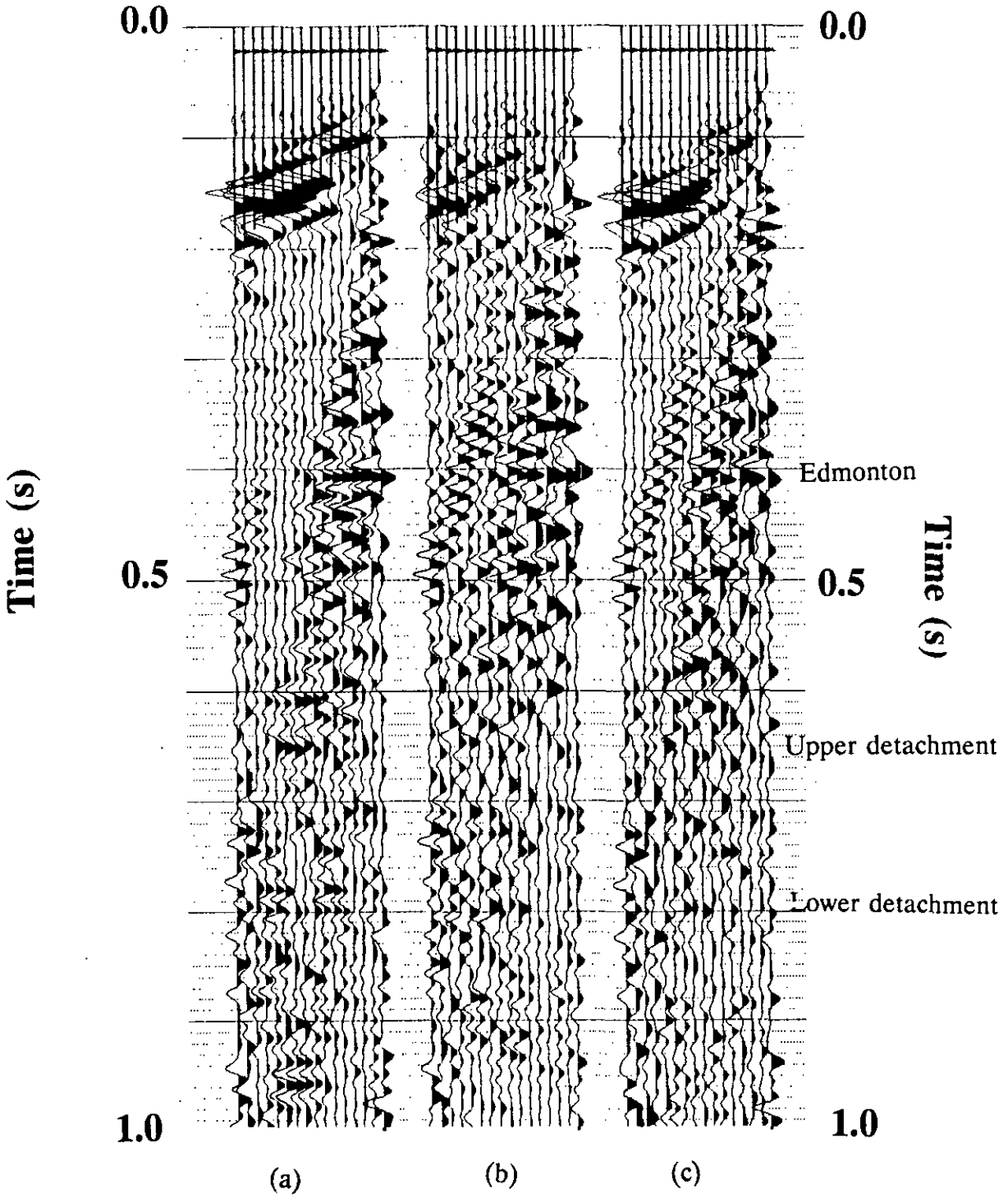

Figure 19 Common offset stacks at station 227, a) after LMF and median f-k filters, b) after LMF and f-k filters and c) conventional stack without filters.

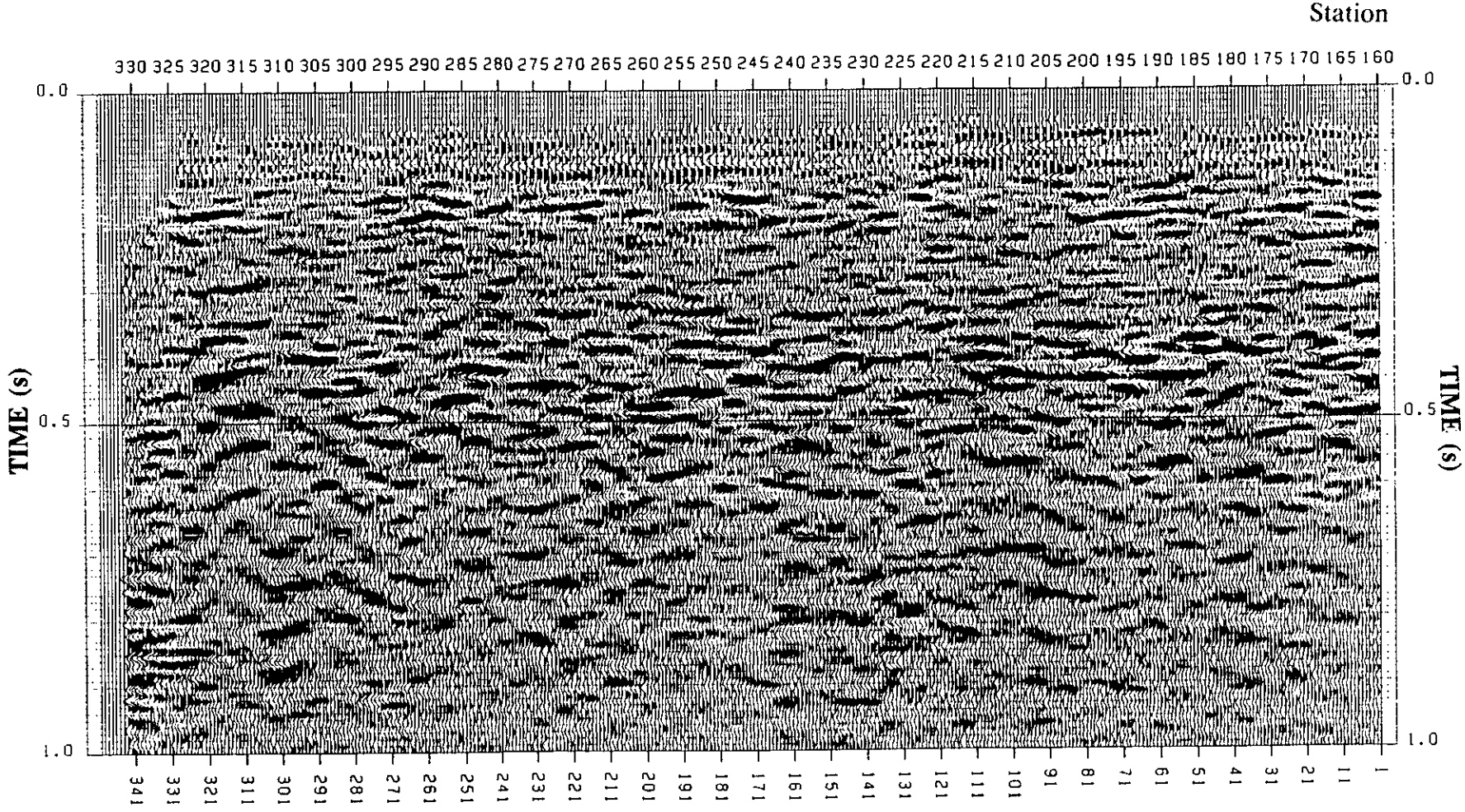

Figure 20 Spring Bank FS91-1 vertical component final stack.

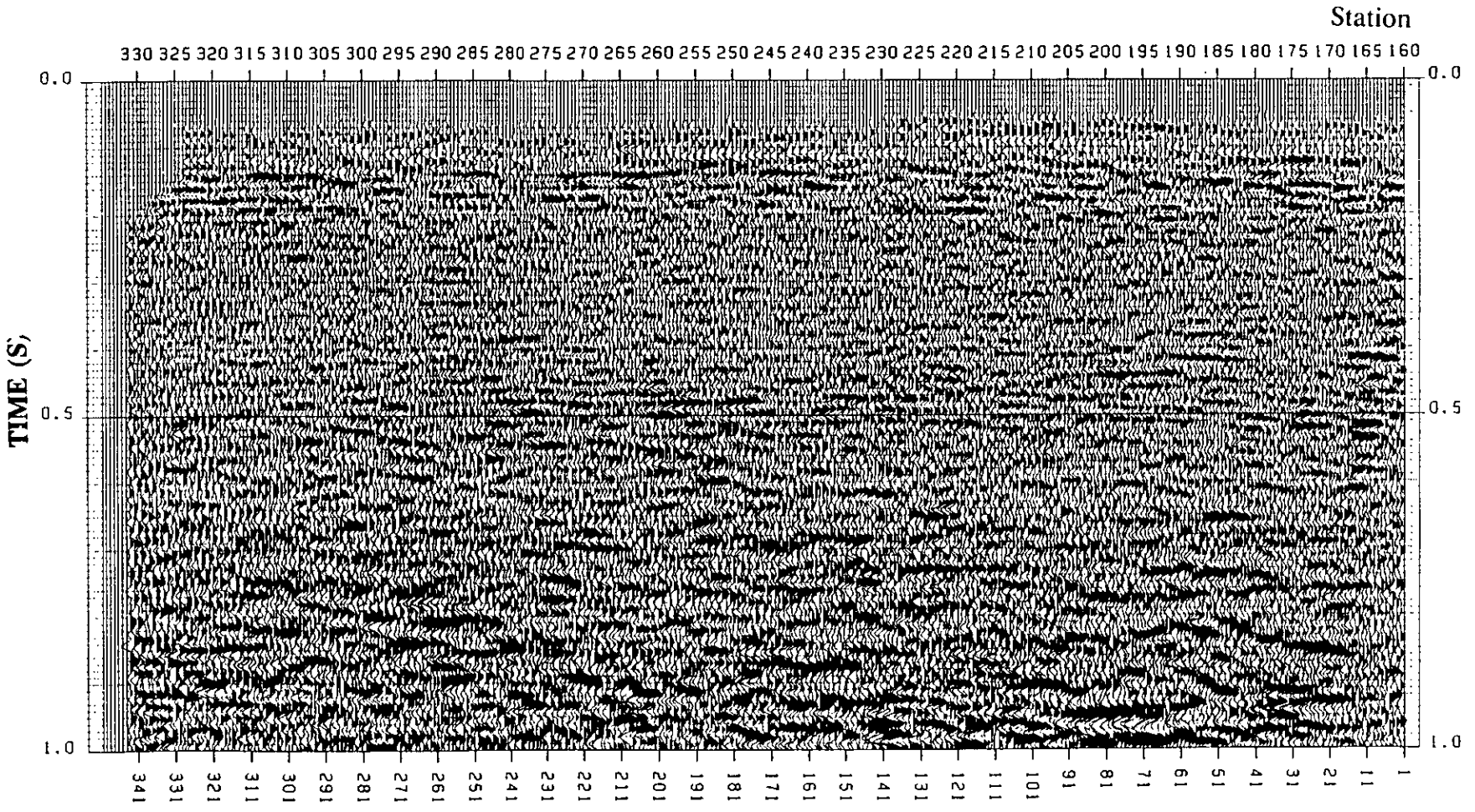

Figure 21 Spring Bank FS91-1 vertical component final stack with inside mute.

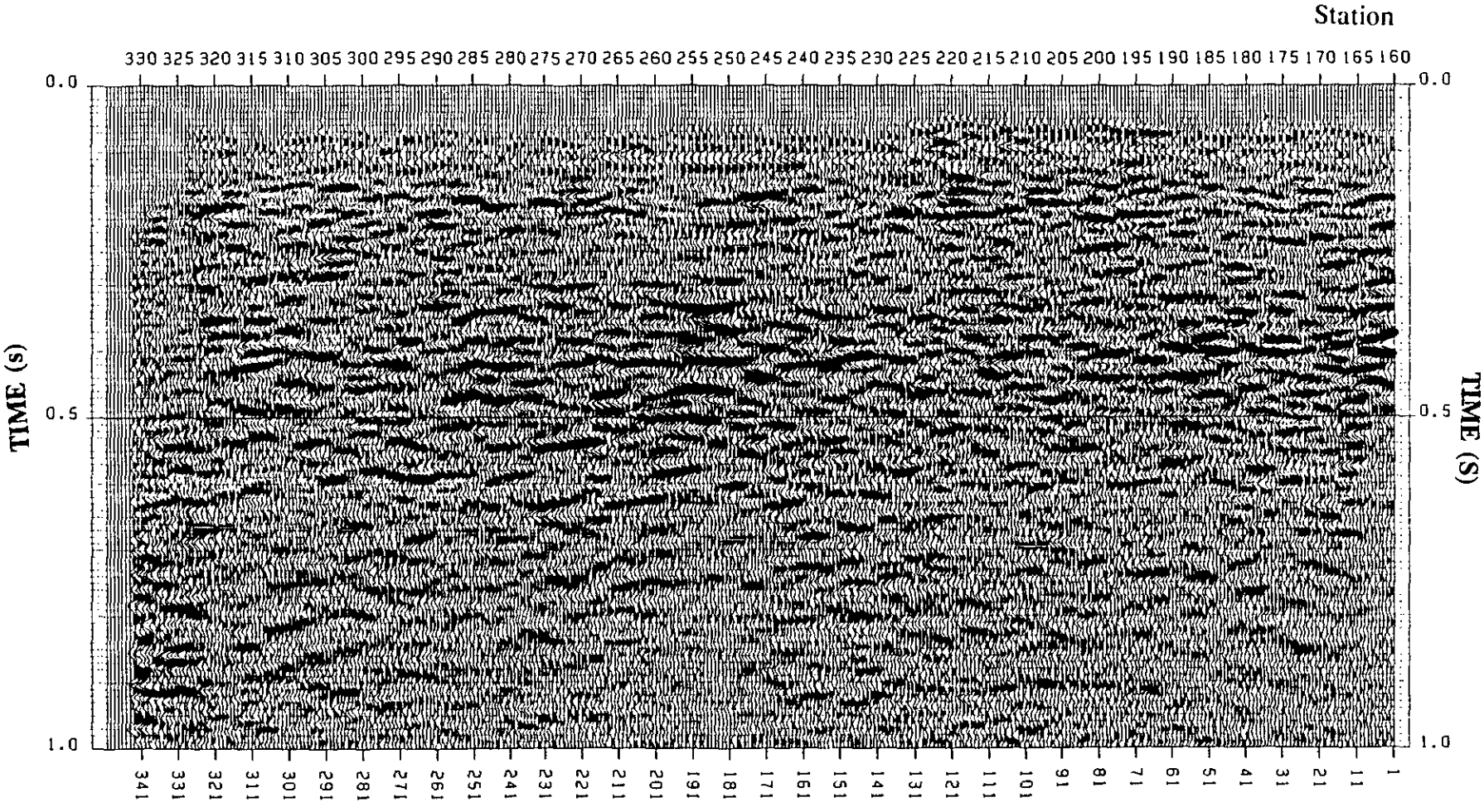

Figure 22 Spring Bank FS91-1 vertical component final stack with LMF compression and pre-stack f-k filters.

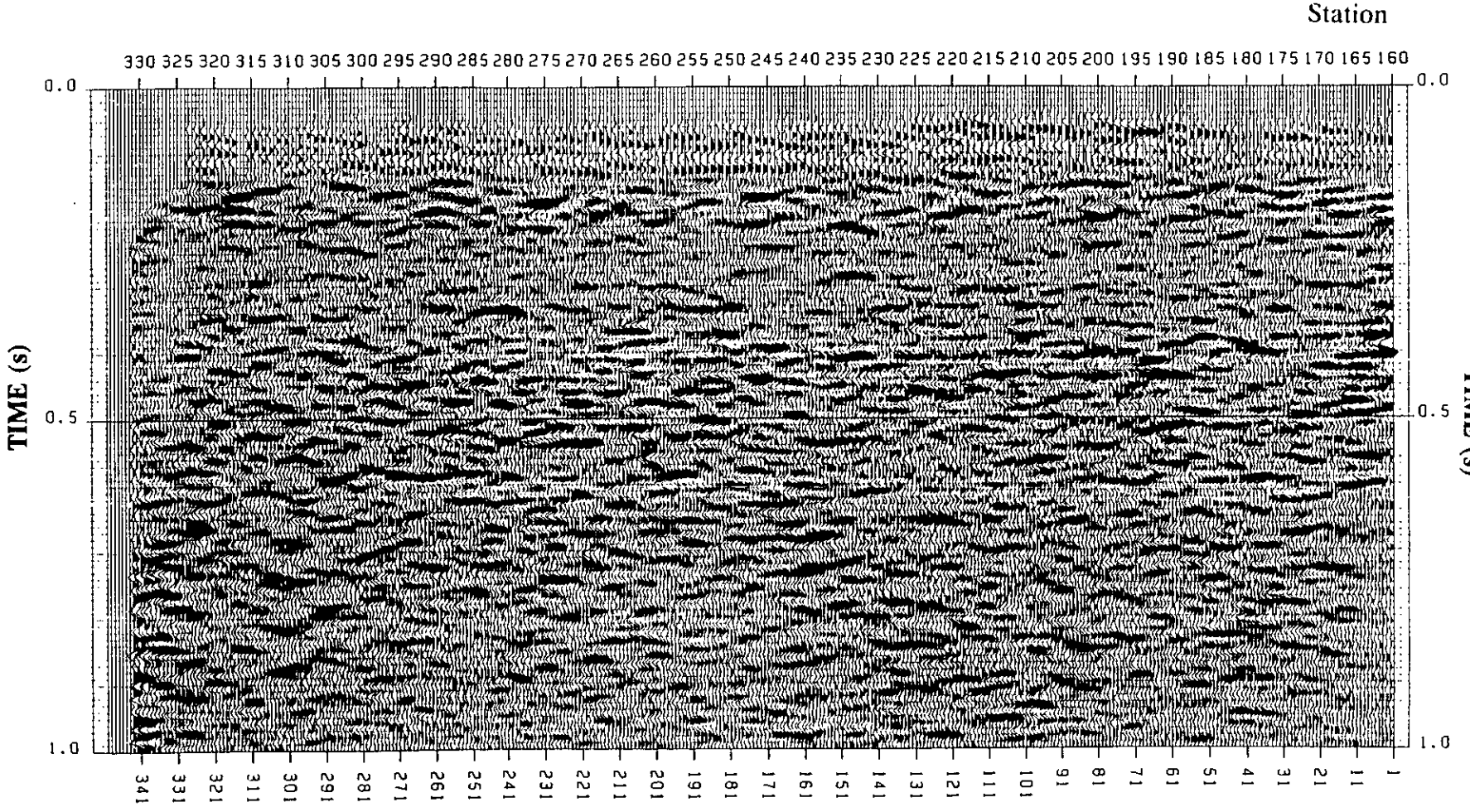

Figure 23 Spring Bank FS91-1 vertical component final stack with LMF compression and pre-stack median f-k filters.

Four final stacks were made to attempt to image these reflectors and compare the ability of these new hybrid multi-channel filters in removing ground roll. Figure 20 and 21 are vertical component stacks without pre-stack filtering. Figure 21 has an inside mute applied designed specifically to remove all ground roll noise with an apparent velocity less than 260 m/s. The resulting stack is still considerably better than the optimum offset single fold stacks used in shallow reflection engineering by Hunter *et al* (1984) as it benefits from a fold multiplicity of 16 times at 500 ms. The results of applying the LFM compression followed by pre-stack f-k or median f-k filtering (Figures 22 and 23) are not as good as simply muting the inside traces. This is especially true above 700 ms. However the median f-k result has a higher signal-to-noise ratio than both the unfiltered and pre-stack f-k filtered section particularly at the level of the lower detachment (≈800 ms).

CONCLUSIONS

The application of a 1-D linear frequency modulated compression operator before multi-channel filtering of dispersive ground roll enhances the advantages of the median f-k filter. Namely dispersive ground roll can be compressed to a single aliased dip which is more easily filtered with this pre-stack filter. The dispersion of Rayleigh waves is primarily dependent on the near surface S-wave thicknesses and velocities. Estimates of the dispersion parameters can be obtained by interpreting the S-wave refraction first breaks, ground roll apparent velocities on narrow band filter panels, or a multi-channel ω-p transform.

Careful acquisition parameters in the case of P-wave shallow reflection studies can avoid the problem of surface wave noise by staying within the optimum window. However, due to logistical limitations this may not always be possible and some form of ground roll filtering may be required. Converted P-Sv shallow reflection studies are even more limited because the additional time delay due to the slower S-wave travel times reduces the available optimum window within which adequate signal-to-noise ratios can be obtained.

ACKNOWLEDGEMENTS

The data was collected thanks to the staff and students participating in the 1991 University of Calgary Geophysics field school. The support of the sponsors of the CREWES project is very much appreciated.

REFERENCES

Abo-Zena, A., 1979, Dispersion function computations for unlimited frequency values: Geophys. J.R. astr. Soc. 58, 91-105.

Aki, K., and Richards, P.G., 1980, Quantitative Seismology: W.H. Freeman and Company, Vol. 2.

Al-Husseini, M.I., Glover, J.B., and Barley, B.J., 1981, Dispersion patterns of ground roll in eastern Saudi Arabia: Geophys. 46, 121-137.

Dobrin, M.B., Simon, R.F., and Lawrence, P.L., 1951, Rayleigh waves from small explosions: Transactions of the Am. Geophys. Union, 32, 822-832.

Doornbos, D.J., 1988, Seismological algorithms: Academic Press Ltd. San Diego, CA., 317-319.

Dziewonski, A.M., and Hales, A.L., 1972, Numerical analysis of dispersed surface waves *in* Methods in computational physics. Vol. 11, *ed* Bolt, B.A., Academic Press.

Gabriels, P., Snieder, R., and Nolet, G.,1987, In situ measurements of shear-wave velocity in sediments with higher-mode rayleigh waves: Geophys. Prosp. 35, 187-196

Glangeaud, F., 1990, Surface wave identification and filtering in multicomponent seismics: presented at the 60th Annual International Meeting, Soc. Expl. Geophys., San Fransisco.

Hunter, J.A., Pullen, S.E., Burns, R.A., Gagne, R.M., and Good, R.L., 1984, Short note - Shallow seismic reflection mapping of the overburden-bedrock interface with the engineering seismograph- some simple techniques: Geophysics, 49, 1381-1385.

Herrmann, R.B., and Russell, D.R., 1990, Ground roll: Rejection using adaptive phase-matched filters: Geophys., 55, 776-781.

Knopoff, L., 1952, On Rayleigh wave velocities: Bull. of the Seism. Soc. of Am., 42, 37-308.

Lawton, D., and Harrison, M.P., 1990, A two-component reflection seismic survey, Springbank, Alberta: CREWES Project Research Report, Vol. 2, 123-163.

Mari, J.L., 1984, Estimation of static corrections for shear-wave profiling using the dispersion properties of Love waves: Geophys. 49, 1169-1179.

McMechan G.A., and Yedlin, M.J., 1981, Analysis of dispersive waves by wavefield transformation: Geophys. 46, 869-874.

Mooney, H.M., and Bolt, B.A., 1966, Dispersive characteristics of the first three Rayleigh modes for a single surface layer: Bull of the Seism. Soc. of Am. 56, 43-67.

Russell, D.R., 1987, Multi-channel processing of dispersed surface waves: Ph. D. Thesis, Saint Louis University.

Saatçilar, R., and Canitez, N., 1988, A method of ground roll elimination: Geophys. 53, 346-358.

Schieck, D.G., and Stewart, R.R., 1990, Pre-stack median f-k filtering: CREWES Project Research Report, Vol. 2, 166-186.

Schwab, F.A., and Knopoff, L., 1972, Fast surface wave and free mode computation *in* Methods in computational physics. Vol. 11, *ed* Bolt, B.A., Academic Press.

Szelwis, R., and Behle, A., 1987, Shallow shear-wave velocity estimation from multimodal rayleigh waves: Shear wave exploration, Soc. Expl. Geophys., Tulsa, 214-226.

Takeuchi, H. and Saito, M., 1972, Seismic surface waves. Methods in Computational Physics, Vol. 11 (ed B.A. Bolt), Academic Press, New York, 217-295.

Tolstoy, I., and Usdin, E., 1953, Dispersive properties of stratified elastic and liquid media: A ray theory: Geophys. 18, 844-870.

Turin, G.L., 1960, An introduction to match filters: IRE Trans., 6, 311-329.

Wattrus, N.J., 1989, Inversion of ground roll dispersion for near-surface shear-wave velocity variations: presented at the 59th Annual International Meeting, Soc. Expl. Geophys., Dallas.